

Effect of Metal Nanoparticles in the Field Emission of Silicon Nanowires

Karanam Madhavi, N. Hanumantha Raju, M. C. Basappa and V. C. Veeranna Gowda*

Department of Physics, Maharani Cluster University, Bengaluru – 560001, Karnataka, India;
vvcvgowda@gmail.com

Abstract

In this work, an efficient method is reported for creating a metal nanoparticle (silver) / Si composite structure consisting of a vertical array of silicon nanowires (SiNWs) decorated with silver metal nanoparticles. A two-stage metal-assisted etching method is employed to obtain SiNWs and Silver (Ag) metal nanoparticles are decorated on the SiNWs using the electroless deposition method. It allows the good coverage of silver metal nanoparticles over SiNWs. Scanning Electron Microscopy (SEM) analysis revealed that Ag was covered with SiNWs. High-work function metal nanoparticles such as Ag nanoparticles on SiNWs have been utilized in different applications such as photovoltaics and sensors. The size of SiNWs is determined through the Raman shift. The silicon optical phonon peak showed an increase in redshift and a decrease of full-width at half maxima with a decrease in diameter due to the quantum confinement. The Electron Field Emission (EFE) characteristics of the Ag-decorated SiNW films were studied based on the current-voltage measurements and analyzed using the Fowler-Nordheim (F-N) equation. The low turn-on field is obtained through the Ag metal nanoparticles which have wider applications in low-power operational devices.

Keywords: Electron Field Emission, Nanowires, Raman Shift, Turn-On Field, Silver Metal

1.0 Introduction

Nanostructures such as Nanowires (NWs), Nanoparticles (NPs), Nanorods (NRs), and nanotubes have attracted increasing attention in a diverse array of nanodevice-related applications due to their fascinating physical and chemical properties¹. The properties of SiNWs can be modified through a Heterostructure Approach (HS)². Among different HS approaches, metal nanoparticle HS is very prominent in different applications³. SiNWs/noble metal Nanoparticle (NP) HS facilitate excellent photocatalytic properties⁴. Metal NP decorated SiNWs have been investigated for different applications such as bio-chemical, and gas sensing applications. A variety of nanoparticles are decorated on SiNWs such as silver (Ag), Gold (Au), and Platinum (Pt) and are studied in

different applications. Among all the metals, Ag is the most effective material for the multifunctional SiNW HS⁵. The synthesis of Ag-decorated SiNWs is an easy and cost-effective and efficient process and its utilization in different areas of nano technology is very effective. Thus Ag@SiNWs is preferred compared to SiNWs. The Raman spectra of nanostructures have become a powerful tool in determining the size of the nanostructures⁶. When the phonons are confined in nanostructures, the translational symmetry gets disturbed and does not obey the conservation of momentum. This produces the asymmetric broadening and hence the Raman shift⁷. Ag @SiNW size is calculated using Raman shift by the Bond Polarizability Model (BPM)⁸. Field emission is considered one of the interesting phenomena in the field of science and technology which depends on the size of the material.

*Author for correspondence

Field emission properties of many other nanomaterials like carbon nanotubes⁹, titanium dioxide nanotubes¹⁰, and tin oxide nanotubes¹¹ have been studied over the past few years. In Field emission science, many methods have been reported to enhance the field emission properties of Carbon Nanotubes (CNT). One of these methods is the Attachment of metal/metal oxide nanoparticles for reducing the work function and the addition of new energy levels near the Fermi energy level (E_f)¹²⁻¹⁴. Chen *et al.*, demonstrated the improvement in the field emission current density by reducing the contact resistance between the substrate and SWCNTs by constructing the Ag nanoparticles¹⁵. SiNWs are good field emitters that have promising applications in cold cathode electron devices and microwave devices¹⁶. Thus, in our work, We have incorporated Ag metal nanoparticles on SiNWs to study the field emission.

In this work, we have fabricated Ag-decorated SiNWs by a typical Metal-Assisted Chemical Etching (MACE) process using Ag as the noble metal catalyst and HF/H₂O₂ as the etchant. The size of Ag-decorated SiNWs has been studied through SEM analysis and Raman spectroscopy Later we studied the electron field emission in Ag-decorated SiNWs.

2.0 Methodology

The cleaned silicon samples have been used to synthesize SiNWs by the MACE method. It begins with pre-immersion treatment. In the pre-immersion treatment, the cleaned silicon wafers are immersed in H₂SO₄ and H₂O₂ solution of a ratio of 3:1 for 10 mins followed by rinsing with deionized water. After pre-immersion treatment, the Ag-nanoparticles were deposited on the silicon wafer by immersing silicon samples in the aqueous solution comprising 0.02 M AgNO₃ and 4.8 M HF for 40 sec. These Ag-deposited silicon wafers were dipped in an etching bath consisting of HF and H₂O₂ for different etching times 45 min, 60 min, and 90min followed by immersion in nitric acid and then in 5% HF-solution to remove the native oxides on silicon wafers respectively. After the fabrication process, the SiNW samples are rinsed with de-ionized water and dried¹⁷. To decorate Ag nanoparticles on SiNWs, the samples were dipped in an aqueous solution of 0.02M AgNO₃ and 4.8M HF for 1

minute in the dark. The morphology and cross-section of the prepared SiNWs are studied using SEM (JSM-6701F, JEOL). The field-emission properties of SiNWs were analyzed in a vacuum chamber with a base pressure of 1×10^{-5} Pa. The distance between the sample and electrode is calculated by digital micrometer and in our work, it is adjusted to 100 μ m. The bias is applied between anode and sample and EFE properties are studied by Keithley-electrometer¹⁸.

3.0 Results and Discussion

SEM images in Figure 1 illustrate the morphology and cross-section of fabricated SiNW samples after an etching time of 45 min. Figure 1(a) shows the morphology of the SiNW sample which consists of pores that are conglomerated. To understand the real structure of SiNWs, a cross-sectional SEM image was taken as shown in Figure 1(b). The cross-sectional image

shows that SiNWs are vertically aligned and they are uniformly distributed on the entire surface of the sample. Figure 1(c) is the cross-section image of Ag-decorated SiNWs. Both cross-section images reveal that the nanowire must be a combination of submicron nanowires. Thus, the actual size of SiNW should be less than how it appears in SEM image which can be investigated using Raman spectroscopy¹⁹. The mechanism for the formation of Ag decorated SiNWs is as follows: When the Ag deposited silicon is placed in an etching solution consisting of HF/H₂O₂/H₂O, silicon beneath the Ag particle dissolves in the solution and the Ag nanoparticle will sink in the holes and their sinking tracks will look like porous silicon and walls of pores left Ag nanoparticles constitute 1D Silicon nanowires. As the etching time increases the sinking track length of Ag nanoparticle increases and hence SiNW length increases¹⁷. After the synthesis of SiNWs, silver nanoparticles are decorated on the surface of SiNWs through electroless deposition. The Ag decoration is preferred on SiNWs to increase the conductivity and to enhance the field emission in different applications.

Raman spectra from bare-Si and etched samples of 45 mins, 60 mins, and 90 mins are shown in Figure 2 (a-d) respectively. Raman spectrum from the bare-Si is centred at 520 cm⁻¹ with FWHM of 3.71 cm⁻¹ as shown in Figure 2(a). Raman spectra from samples of

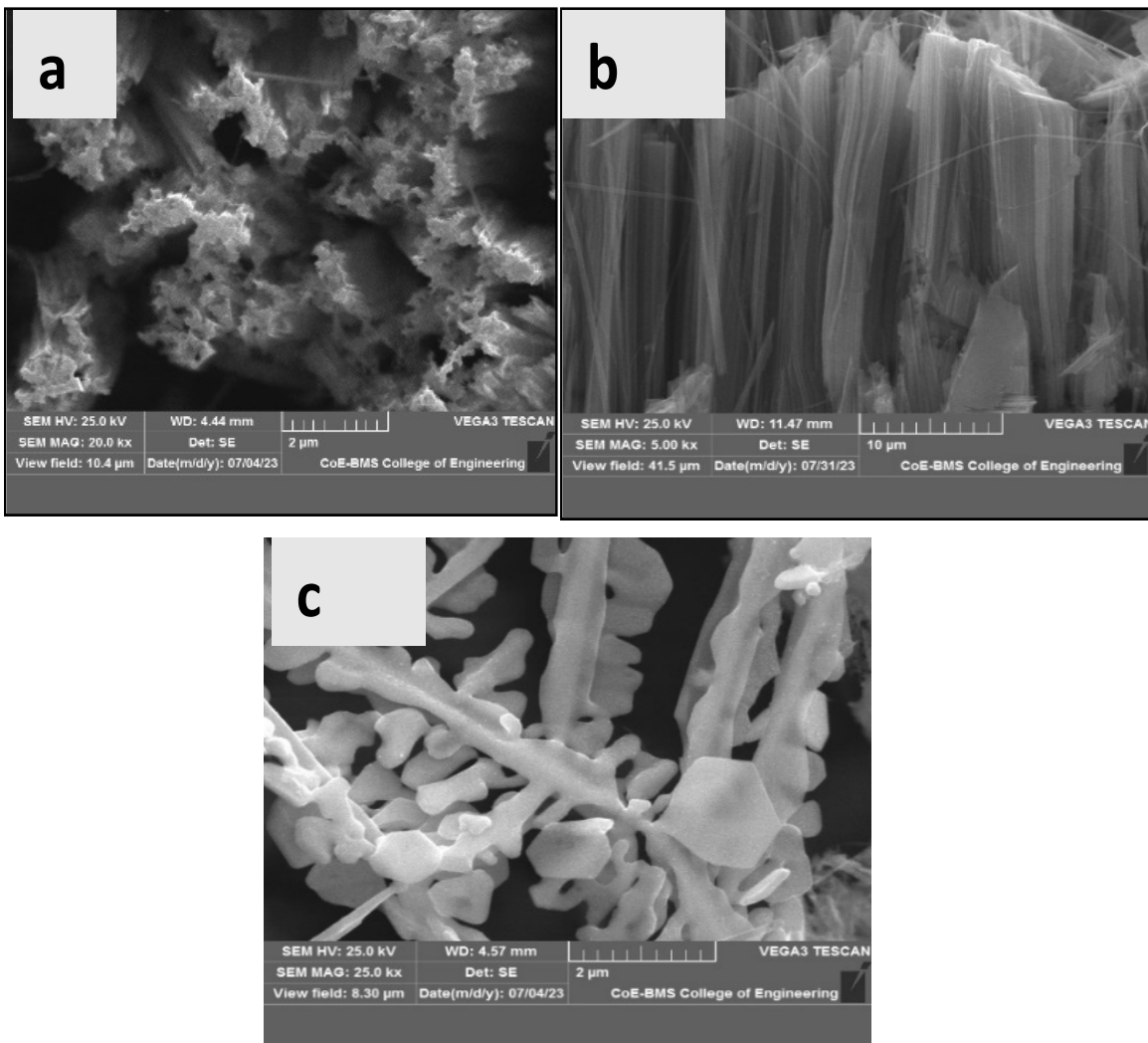


Figure 2. SEM images of SiNWs grown using MACE (a) Morphology of SiNWs. (b) Cross section of SiNWs after etching time 45 mins. (c) Ag decorated SiNWs.

45 mins, 60 mins, and 90 mins are shown in Figure 2(b, c, d), respectively. Raman spectra of these samples show the following variations with increasing etching time. (1) The Raman peak of the SiNWs is red-shifted as compared to the usual Raman active optical mode of bare-Si (i.e., 520 cm⁻¹). Raman peak shifts gradually from 520 cm⁻¹ to 515.0 cm⁻¹ as the etching time is increased from 45 mins to 90 mins (2) As the etching time is increased, the Raman spectra of SiNWs are broadened compared to bare-Si and asymmetric nature increased with etching time. (3) Raman spectra get broadened in comparison to that of the bare-Si. The results from Raman spectra can be explained based on the quantum confinement effect. As

the etching time is increased, the Raman peak is shifted towards the lower frequency side and asymmetry in the shape of the curve is increased. Thus Raman shift is a function of SiNW size. The SiNW size can be estimated through the BMP model given by

$$\Delta\omega = \omega(L) - \omega(0) = -A \left(\frac{a}{L}\right)^\gamma \tag{1}$$

where, L gives the size of SiNWs, Δω is the Raman shift, A=20.92 cm⁻¹ and γ=1.08 have taken from previous reports⁸ and a=Lattice constant of silicon = 5.43 cm³. The size of the SiNWs is calculated using Equation (1). The results from Raman spectra and SiNWs size are shown

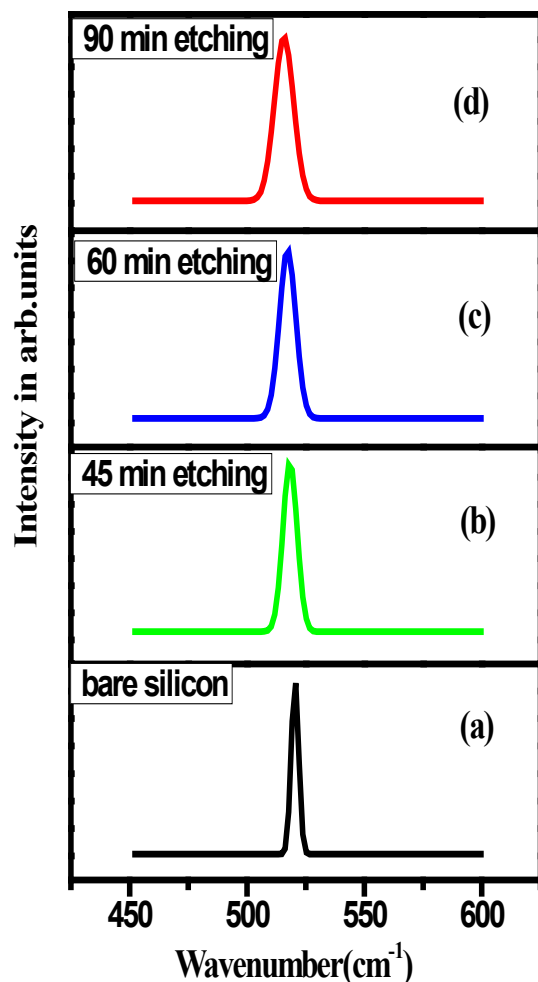


Figure 2. Raman spectra of SiNWs (a) bare silicon (b) 45 mins etched sample (c) 60 mins etched sample (d) 90 mins etched sample.

in Table 1. It is observed that the Full-width half maxima is increased and the size of SiNWs is decreased with the increase of etching time. After an etching time of 90 mins, the SiNW size is decreased to 24.85 nm. The decrease in the size of SiNWs will enhance the electron field emission. Thus 90-minute etched sample which is decorated with Ag metal nanoparticles has opted for Field emission measurements.

The EFE measurements have been carried out at room temperature. Figure 3(a) shows the I-V characteristics of S_1 , S_2 and S_3 at 45 min and 90 min. S_2 and S_3 are the SiNWs sample and Ag decorated SiNWs sample respectively after 90 min etching time. The emission current is noted as a function of the applied voltage from 0 V to 1200 V. The Turn-on field (the field required to detect a current of 0.01 mA/cm²) is calculated from the I-V data. It was found to be 9.55 V/ μ m and 6.08 V/ μ m for the S_2 and S_3 samples respectively.

The turn on-field is decreased in the S_3 sample. This is because the work function of silicon is decreased due to the incorporation of Ag metal nanoparticles on the SiNWs. As a result, the structural and electronic properties are modified and the potential barrier is reduced which promotes the quantum tunnelling of electrons at low turn-on field²⁰. The other EFE parameter is the field enhancement factor be determined by F-N equation²¹, i.e.,

$$I = \frac{aE_{effe}^2}{\phi} \exp\left(-\frac{b\phi^{3/2}}{E_{effe}}\right) \quad (2)$$

where, a and b are constants that depend on the work-function ϕ of the material. For silicon $a = -1.54 \times 10^{-3}$

Table 1. Raman shift, Silicon nanowire (SiNW) size and FWHM at different etching times

Sample	Raman Shift	SiNW size nm	FWHM cm ⁻¹
Bare silicon	--	----	3.71
45 min etched silicon	2.2	54.73	7.16
60 min etched silicon	3.7	33.82	8.24
90 min etched silicon	5.16	24.85	9.64

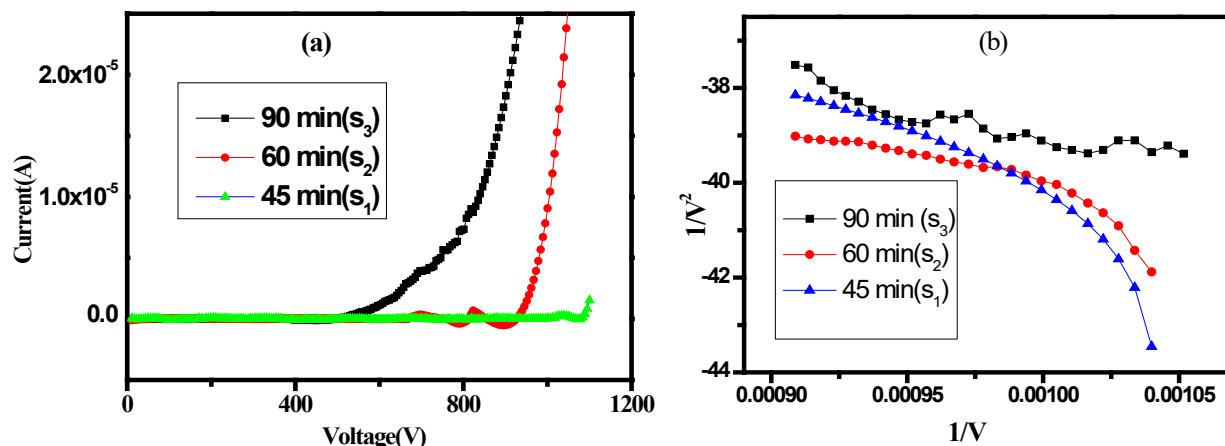


Figure 3. (a) I-V characteristics of SiNWs, (b) F-N plot of SiNWs.

Table 2. Field emission parameters of SiNWs

Sample	Size of Nanowire (nm)	Turn on field V/μm	Field enhancement factor ()
S ₁	54.73	---	303
S ₂	33.82	9.55	394
S ₃	24.85	6.08	524

A $eV V^{-2}$ and $b=6.83 \times 10^3 eV^{-3/2} \mu V^{-1}$, E_{eff} is the effective electric field, $E_{eff} = \beta E_0$, where β is field-enhancement factor and $E_0 = V/d$ is the average effective electric-field, V is the voltage applied, d is the distance between silicon nanowire tip and anode. Then F-E equation can be written as

$$\ln\left(\frac{I}{V^2}\right) = \ln\left(\frac{a\beta^2}{\phi d^2}\right) - \frac{b\phi^{3/2} d}{\beta V} \quad (3)$$

Plotting $\ln\left(\frac{I}{V^2}\right)$ versus $\left(\frac{1}{V}\right)$ yields a straight line which is called F-N plot with the slope of $\left(-\frac{b\phi^{3/2} d}{\beta V}\right)$ and with the intercept of $\ln\left(\frac{a\beta^2}{\phi d^2}\right)$ ²²

Figure 3(b) displays the F-N plots of SiNWs. The field enhancement factor β was calculated from the slope, where slope = $-\frac{b\phi^{3/2} d}{\beta}$, where $\phi = 4.15 eV$, $d = 100 \mu m$, $b = -6.83 \times 10^3 eV^{-3/2} \mu m^{-1}$. The field enhancement factor β

for s1, s2 and s3 are 303.5, 339.16 and 524, respectively. The enhancement in the β shows superior EFE quality. The enhancement of β in Ag decorated SiNWs due to the addition of new energy levels near the fermi energy level which modifies the density of states through Ag metal nanoparticles²². Thus, low turn-on field and enhancement of field emission factor are the evidence to believe that Ag metal nanoparticle decoration on SiNWs could improve the electron field emission property of SiNWs. The electron field emission parameters attained from the F-N plots are listed in Table 2.

4.0 Conclusions

Metal-assisted chemical etching provides a simple approach to prepare SiNWs. Ag metal nanoparticles are decorated on SiNWs by electroless method. It is observed from the SEM images that the vertically aligned SiNWs are formed along the whole surface of the silicon wafer. Raman analysis measurements were carried out to

measure the size of SiNWs at different etching times by the BPM model. It was found that SiNWs size decreased with the increase in etching time. electron field emission measurement had been carried out in Ag-decorated SiNWs. A low turn-on field of $6.5\text{V}/\mu\text{m}$ and enhancement of β from 339 to 524 is achieved in Ag decorated SiNWs. Further optimization of parameters may lead to improvement in the EFE properties.

5.0 References

- Otto M, Algasinger M, Branz H, Gesemann B, Gimpel T, Füchsel K, *et al.* Black Silicon Photovoltaics. *Adv Optical Mater.* 2015; 3(2):147-64. <https://doi.org/10.1002/adom.201400395>
- Ghosh R, Ghosh J, Das R, Mawlong LPL, Paul KK, Giri PK. Multifunctional Ag nanoparticle decorated Si nanowires for sensing, photocatalysis and light emission applications. *J Colloid Interface Sci.* 2018; 53:464-73. <https://doi.org/10.1016/j.jcis.2018.07.123> PMID:30099309
- Fang C, Agarwal A, Widjaja E, Garland MV, Wong SM, Linn L, *et al.* Metallization of Silicon Nanowires and SERS response from a single metallized nanowire. *Chem Mater.* 2009; 21(15):3542-8. <https://doi.org/10.1021/cm900132j>
- Liao F, Wang T, Shao M. Silicon nanowires: Applications in catalysis with distinctive surface property, *J Mater Sci: Mater Electron.* 2015; 26(7):4722-9. <https://doi.org/10.1007/s10854-015-2949-8>
- Paul KK, Ghosh R, Giri PK. Mechanism of strong visible light photocatalysis by Ag_2O nanoparticle-decorated monoclinic $\text{TiO}_2(\text{B})$ porous nanorods. *J Nanotechnology.* 2016; 27(31):315703-3. <https://doi.org/10.1088/0957-4484/27/31/315703> PMCID:PMC9794414
- Kumar V, Saxena K, Shukla AK. Silicon nanowires prepared by Metal Induced Etching (MIE): Good field emitters. *IET Micro Nano Lett.* 2013; 8:311-14. <https://doi.org/10.1049/mnl.2012.0910>
- Richter H, Wang ZP, Ley L. The one phonon Raman spectrum in microcrystalline silicon. *Solid State Commun.* 1981; 39:625-9. [https://doi.org/10.1016/0038-1098\(81\)90337-9](https://doi.org/10.1016/0038-1098(81)90337-9)
- Zi J, Büscher H, Falter C, Ludwig W, Zhang K, Xie X. Raman shifts in Si nanocrystals. *Appl Phys Lett.* 1996; 69:200-2. <https://doi.org/10.1063/1.117371>
- Kyung S-J, Lee Y-H, Kim C-W, Lee J-H, Yeom G-Y. Field emission properties of carbon nanotubes synthesized by capillary type atmospheric pressure plasma enhanced chemical vapor deposition at low temperature. *J Carbon.* 2006; 44:1530-4. <https://doi.org/10.1016/j.carbon.2005.12.020>
- Antony RP, Mathews T, Panda K, B Sundaravel, Dash S, Tyagi AK. Enhanced field emission properties of electrochemically synthesized self-aligned nitrogen-doped TiO_2 nanotube array thin films. *J Phys Chem.* 2012; 116(31):16740-6. <https://doi.org/10.1021/jp302578b>
- Deshpande AC, Koinkar PM, Ashtaputre SS, More MA, Gosavi SW, Godbole PD, *et al.* Field emission from oriented tin oxide rods. *Thin Solid Films.* 2006; 515(4):1450-4. <https://doi.org/10.1016/j.tsf.2006.04.034>
- Sreekanth M, Ghosh S, Biswas P, Kumar S, Srivastava P. Improved field emission from indium decorated multi-walled carbon nanotubes. *Appl Surf Sci.* 2016; 383:84-9. <https://doi.org/10.1016/j.apsusc.2016.04.170>
- Sridhar S, Tiwary C, Vinod S, Taha-Tijerina JJ, Sridhar S, Kaushik K, *et al.* Field emission with ultralow turn on voltage from metal decorated carbon nanotubes. *ACS Nano.* 2014; 8:7763-70. <https://doi.org/10.1021/nn500921s> PMID:25054222
- Gautier L-A, Le Borgne V, Delegan N, Pandiyan R, El Khakani MA. Field electron emission enhancement of graphenated MWCNTs emitters following their decoration with Au nanoparticles by a pulsed laser ablation process. *Nanotechnology.* 2015; 26(4). <https://doi.org/10.1088/0957-4484/26/4/045706> PMID:25567743
- Chen L, Wang L, Yu X, Zhang S, Li D, Xu C, *et al.* Constructing Ag nanoparticles-single wall carbon hybrid nanostructure to improve field emission properties. *Appl Surf Sci.* 2013; 265:187-91. <https://doi.org/10.1016/j.apsusc.2012.10.164>
- Huang CT, Hsin CL, Huang KW, Lee CY, Yeh PH, Chen US, *et al.* Field emission enhancement of Au-Si nanoparticle-decorated silicon nanowires. *Appl Phys Lett.* 2007; 91. <https://doi.org/10.1063/1.2777181>
- Madhavi K, Suvarna RP, Ghosh M, Shaik H, Rao GM. Effect of plasma ion etching towards super-hydrophobicity. *J. Mater.* 2016; 3:1907-13. <https://doi.org/10.1016/j.matpr.2016.04.091>
- Sahoo SK, Marikani A. Morphological dependence of field emission properties of silicon nanowire

- arrays. *J Nano*. 2016; 11(02). <https://doi.org/10.1142/S179329201650017X>
19. Kumar V, Saxena SK, Kaushik V, Saxena K, Shukla AK, Kumar R. Silicon nanowires prepared by Metal Induced Etching (MIE): Good field emitters. *RSC Adv*. 2014; 4. <https://doi.org/10.1039/C4RA11093E>
20. Raza MMH, Aalam SM, Sadiq M, Sarvar M, Zulfequar M, Husain S, *et al*. Study the electron field emission properties of silver nanoparticles decorated carbon nanotubes-based cold-cathode field emitters via post-plasma treatment. *J Mater Sci Mater Electron*. 2022; 33: 7191-211. <https://doi.org/10.1007/s10854-022-07900-y>
21. de Heer WA, Ch telain A, Ugarte D. Carbon nanotube field-emission electron source. *J Science*. 1995; 270:1179-80. <https://doi.org/10.1126/science.270.5239.1179>
22. le Fèvre AJ, Abelmann L, Lodder JC. Field emission at nanometer distances for high-resolution positioning. *J Vac Sci Technol*. 2008; B(26):724-9. <https://doi.org/10.1116/1.2894898>